IOPscience iopscience.iop.org

Home Search Collections Journals About Contact us My IOPscience

Application of high-resolution x-ray diffraction for detecting defects in SiGe(C) materials

This article has been downloaded from IOPscience. Please scroll down to see the full text article.

2005 J. Phys.: Condens. Matter 17 S2315

(http://iopscience.iop.org/0953-8984/17/22/020)

View the table of contents for this issue, or go to the journal homepage for more

Download details:
IP Address: 129.252.86.83
The article was downloaded on 28/05/2010 at 04:55

Please note that terms and conditions apply.

INSTITUTE OF PHYSICS PUBLISHING JOURNAL OF PHYSICS: CONDENSED MATTER

J. Phys.: Condens. Matter **17** (2005) S2315–S2322 doi:10.1088/0953-8984/17/22/020

Application of high-resolution x-ray diffraction for detecting defects in SiGe(C) materials

Henry H Radamson and Julius Hållstedt

Royal Institute of Technology (KTH), Department of Microelectronics and Information Technology (IMIT), Electrum 229, Kista-Stockholm, S-164 40, Sweden

E-mail: rad@imit.kth.se

Received 6 October 2004, in final form 15 February 2005
Published 20 May 2005
Online at stacks.iop.org/JPhysCM/17/S2315

Abstract
The application of high-resolution x-ray diffraction for detecting and distinguishing defects in SiGe(C) layers is presented. A depth profile of the defects in SiGe/Si multilayers has been performed by using high-resolution reciprocal lattice mapping at different asymmetric reflections. Transmission electron microscopy was also applied in order to observe defects in the layers and these results were linked with the x-ray analysis. The substitutional C or B concentration in SiGe was measured by the shift of layer peak compared to the intrinsic layers. The thermal stability of the SiGe layers was investigated in order to rank the epitaxial quality of the SiGe below the detection limit of x-ray technique. It has also been demonstrated that x-ray analysis can be used for in-line process monitoring of layers grown in small device openings on patterned substrates. These types of analysis have also been used routinely for the evaluation of processed samples.

1. Introduction

In recent years, mismatched heterostructures have been integrated in many different types of device applications [1]. The estimation of defect density in these layers is an important issue since the defects affect the electrical, optical and mechanical behaviour of these layers. Thus, the necessity of having a precise, fast and cheap characterization technique is inevitable. X-ray techniques have obtained a strong position in this field due to their non-destructive character without any need of sample preparation, and also the possibility to be applied as in-line direct measurements. It is desirable to apply a guide map for the x-ray measurements which makes it easier to evaluate different defects in the epitaxial layers. In this paper, methods to detect and distinguish defects with depth analysis, estimation of substitutional dopant concentration in SiGe(C) layers and also the capability of in-line process monitoring measurements using high-resolution x-ray diffraction are presented.

 © 2005 IOP Publishing Ltd Printed in the UK

2. Experimental details

The SiGe(C) samples in this study were grown on blanket or patterned Si[100] substrates in an ASM Epsilon 2000 RPCVD reactor. High-resolution x-ray diffraction (HRXRD) and high-resolution reciprocal lattice mapping (HRRLM) were performed by using a Philips X'pert instrument with Cu target and Kα_1 ($\lambda = 0.1504$ nm) was obtained from a four-crystal Ge(220) monochromator. By introducing a mirror prior to the monochromator and decreasing the spot size an intense narrow x-ray beam is obtained. In this way, an array of individual single crystalline stacks grown selectively in oxide openings can be analysed. The x-ray beam can be applied to measure the misfit parameters parallel and perpendicular to the growth direction. An HRRLM is a series of $\omega/2\theta$ rocking curves (ω and 2θ are the incident and diffracted beam, respectively) with $\omega \pm \Delta\omega$ as starting incident angle. The compiled file of these rocking curves is illustrated as equi-intensity contours in k-space. The position and shape of layer and substrate peaks provide information about the misfit parameters, strain relaxation and the amount of defect density in the epitaxial layers. A Normarski microscope (combined with wet-etching) has been applied in order to determine the dislocation density in the layers. Transmission electron microscopy (TEM) was used in order to distinguish different types of defects. In the SiGe layers, defects were created by rapid thermal annealing (RTA), applying high doping concentrations and by tuning the growth rate in epitaxial process.

3. Determination of mismatch parameters in the heterostructures

In HRRLMs, the positions of the substrate and layer peak provide the lattice mismatch parameters perpendicular and parallel to the growth direction by using the following the equations:

$$f_\perp = \frac{\sin\theta_s \cos(\omega_s - \theta_s)}{\sin\theta_l \cos(\omega_l - \theta_l)} - 1 \tag{1}$$

$$f_\parallel = \frac{\sin\theta_s \sin(\omega_s - \theta_s)}{\sin\theta_l \sin(\omega_l - \theta_l)} - 1 \tag{2}$$

where the indices s and l stand for the substrate and the layer, respectively [2, 3]. The lattice mismatch can be written:

$$f = (f_\perp - f_\parallel)\frac{1-\upsilon}{1+\upsilon} + f_\parallel \tag{3}$$

where υ is the Poisson ratio ($\upsilon = 0.278$) for $Si_{1-x}Ge_x/Si$ and the incorporation of C in these heterostructures is believed to have only a minor effect on the Poisson value [4]. The widths of the layer and substrate peaks and the low-intensity broadening can provide valuable information about the density and the structure of the defects.

4. Results and discussions

Heterostructures with various doping levels are used for opto- and electro-device applications. In these layers, estimation of substitutional doping concentration is an essential matter. Due to the size difference of the dopant atoms with the host atoms, a strain is often induced in the doped layers. As examples, in SiGeC/Si or B-doped SiGe/Si heterostructures carbon or boron atoms compensate the compressive strain of Ge atoms. The strain compensation amount can be easily measured by HRXRD and can be converted to substitutional carbon or boron concentration in SiGe layers. The non-substitutional dopant atoms in these layers does not contribute to the strain compensation and can thus not be estimated. However, by combining HRXRD with

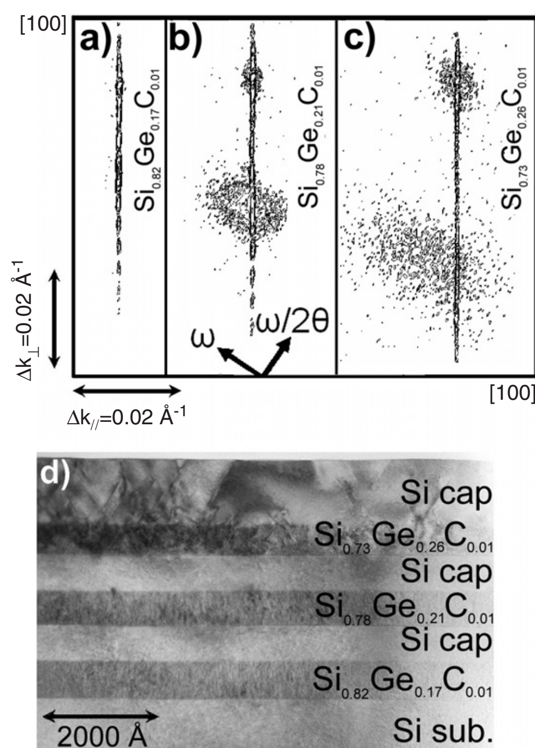

Figure 1. HRRLMs around the (113) reflection of three SiGeC layers with increasing Ge composition. A TEM image with all layers from (a) to (c) is shown in (d).

secondary ion mass spectrometry (SIMS) (which measures the total concentration) the amount of interstitial dopants can be obtained.

A series of SiGeC layers with high carbon concentration were grown to study the incorporation of carbon atoms and evolution of defects in these thin films. HRRLMs of these layers are shown in figures 1(a)–(c) as follows: 1(a) $Si_{0.82}Ge_{0.17}C_{0.01}$, 1(b) $Si_{0.78}Ge_{0.21}C_{0.01}$, 1(c) $Si_{0.73}Ge_{0.26}C_{0.01}$. As a reference sample, all these SiGeC layers were grown in a SiGeC/Si multilayer structure and a cross-sectional TEM of this sample is shown in 1(d). The substrate and SiGeC layer peaks in figure 1(a) are lined up along $K_{\perp}$ with a narrow full width at half maximum (FWHM) indicating a high epitaxial quality. However, a diffused scattering is observed around the layer peak in figures 1(b) and (c), indicating the generation of defects. In these figures, the main contour lines are not affected but the feature of the diffused scattering around the SiGeC layer peaks is quite different. It is more asymmetric in figure 1(c) compared to 1(b). The TEM micrograph shows that the SiGeC layer in 1(c) has extended defects: stacking faults and misfit dislocations; however, the SiGe layer in 1(b) contains no visible defects. The observations by Normarski microscope (the layers were wet-etched stepwise) showed no dislocation cross-hatched pattern for the samples in figures 1(b) and (a). Therefore, we believe that the diffused scattering in figure 1(b) is due to carbon precipitates in the SiGe layer. A similar diffused scattering has been observed previously in the case of B- [5] and C-doped [6] SiGe layers demonstrating two-dimensional precipitates with no dislocations. The main reason for this diffused scattering is that the precipitates create only a local distortion in the lattice.

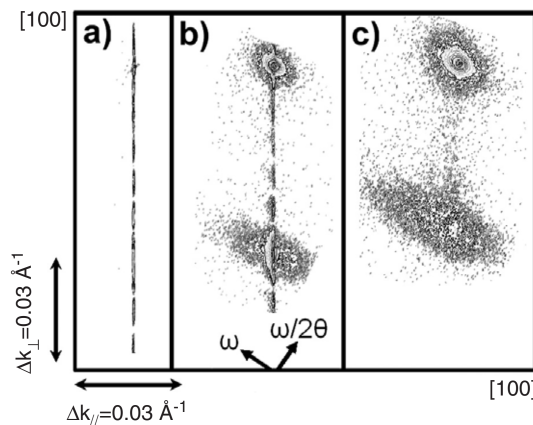

Figure 2. HRRLMs around the (113) reflection of $Si_{0.74}Ge_{0.26}$ samples showing (a) as-grown and RTA treated samples for 10 s at (b) 1050 °C and (c), 1070 °C.

Further analysis was performed in order to distinguish the feature of the misfit dislocation in the HRRLMs compared to stacking faults or precipitates in the SiGe layers. This was performed by studying the thermal stability of the SiGe layers. Figures 2(a)–(c) show HRRLMs of $Si_{0.74}Ge_{0.26}$ layers RTA treated at different temperatures as follows: 2(a) as-grown, 2(b) 10 s at 1000 °C and 2(c) 10 s at 1070 °C respectively. The as-grown sample demonstrates high epitaxial quality, while both the other samples show asymmetric broadening around the layer peaks. In these samples, the low intensity contours become asymmetric and this feature differs from the diffused scattering around the SiGe layer in figure 1(c). For the annealed samples, the position of the layer peak has also shifted because of the strain relaxation. The relaxation amount was calculated to be close to 10% in 2(b) and almost 50% in 2(c).

Thus the above results demonstrate that the defects determine the feature of the layer peaks dependent on their nature or the scale of the relaxation amount. The extended defects such as stacking faults or dislocations cause a strong lattice distortion, whereas the precipitates are locally positioned defects and their existence does not cause large scale damage. It is worth mentioning here that two-dimensional simulations of these HRRLMs is complicated because of the nature of the defects and their distribution in the epitaxial layers.

5. Depth resolution analysis

In a multilayer structure detecting and localizing the defects is an important task. Traditionally TEM analysis has been applied to reveal the defects in the layers. The x-ray technique also offers an opportunity to qualify the epitaxial layers by performing HRRLMs around different asymmetric reflections. The main idea is tuning the penetration depth or the probing volume of the x-ray beam in the samples. Asymmetric reflections, e.g. (113), (224) and (115) with incident angle of 2.8°, 8.7° and 31.7°, respectively, are used to perform depth analysis. Figures 3(a)–(c) illustrate the HRRLMs around these asymmetric reflections from an SiGe/Si multilayer structure in the previously discussed TEM micrograph in figure 1(d). The choice of this sample is a link between TEM with HRRLM results. In this sample, the SiGeC top layer had mainly stacking faults and some dislocations which had also propagated into the Si Cap layer, whereas the intermediate layer contained precipitates and the first SiGeC layer was defect-free. In the HRRLMs in figures 3(a)–(c), there are three SiGe layer peaks lines with

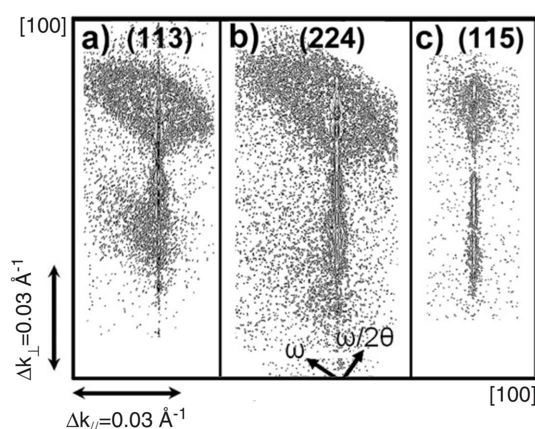

Figure 3. HRRLMs around (113), (224) and (115) reflections of the SiGe/Si multilayer shown in the TEM image in figure 1(d).

some thickness fringes. The diffused scattering around the substrate peak, which is in fact overlapped with the Si substrate peak, reveals the defects in the cap Si layer. This is visible in the (113) and (224) reflections, figures 3(a) and (b), with low incident angle, and is not detectable in the (115) reflection in figure 3(c) in which the x-ray beam penetrates deeper into the substrate with high absorption level. A similar discussion can be applied for revealing defects in the intermediate and cap SiGe layers in the form of diffused scattering around the layer peak in the HRRLMs, and it becomes successively weaker from (113), (224) to (115) reflections. These results indicate that the HRRLMs around (113) are the most sensitive tool for defects situated close to the surface. One important point here is that the layer defect may cause surface roughness. This induces a diffused scattering feature especially in the HRRLM around the (113) reflection. Extra care has to be taken in this case for measurements on III–V materials since the incident beam angle for the (113) reflection is only 1.69°, and the surface morphology may have a dominant effect.

6. The measurement of defect density in epitaxial layers

In previous reports, the x-ray rocking curve technique has been presented as a powerful technique to measure dislocation density in the epitaxial layers [7]. This technique is based on measuring the FWHM of the rocking curves at different reflections. In general, the broadening of the rocking curves in single-crystalline material is due to two main reasons:

(i) the dislocation causes a rotation of the crystal lattice (so-called angular broadening), and
(ii) a distortion of the Bragg angle due to the strain relaxation in the neighbourhood of the dislocations (so-called strain broadening).

This method has been used for different heteroepitaxial semiconductors and it can determine dislocation densities in the range 10^5–10^9 cm^{-2}. In recent years, further improvements in the epitaxial quality have required higher detection sensitivity.

In semiconductor crystals, a range of different types of defects exists and they may interact strongly with each other when they are mobile. This interaction is thermally dependent and can be excited by an RTA process. This theory has been examined for a series of $Si_{0.85}Ge_{0.15}$ samples which were grown with different growth rates. The defect density in the as-grown

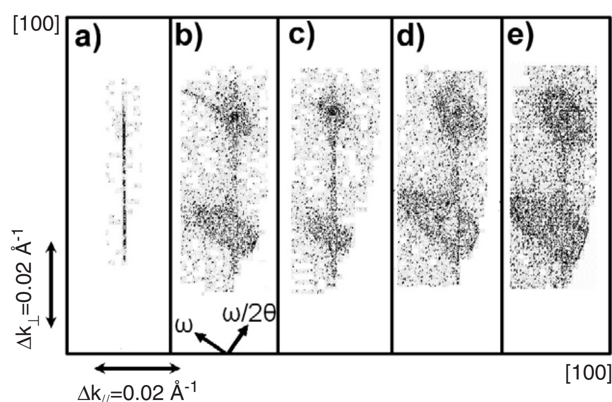

Figure 4. HRRLM around the (113) reflection of a 1200 Å thick $Si_{0.85}Ge_{0.15}$ layers with different growth rates. (a) Illustrates an as-grown example whereas (b)–(e) has been RTA treated at 900 °C for 10 s.

layers was below the detect limit. HRRLMs around the (113) reflection of samples are demonstrated in figures 4(a)–(e) as follows: 4(a) as-grown with 156 Å min^{-1} and samples which were grown with growth rate of 4(b) previous sample, 4(c) 218, 4(d) 368 and 4(e) 392 Å min^{-1} and later RTA treated for 10 s at 900 °C. In this series, the samples with higher defect density demonstrate a lower thermal stability. In this way, there is an opportunity to rank the layers according to the defect density amount. These results show that a too low or high growth rate causes an increase in defect density, and there is an optimum value for deposition of these layers as shown in figure 4(c). The main reason for this behaviour is that the epitaxy process at low growth temperature range is in the kinetic regime, and an increase of partial pressure (amount of the reactant) has only a slight enhancement in the growth rate. This may result in an increase of point defects in the lattice. A similar dependence of defect density in SiGe layers on growth rate has also been observed for Cl-based epitaxy [8].

7. X-ray analysis for in-line process monitoring

Selectively grown SiGe-based material has been used in CMOS structures as the channel layer or in source/drain junctions. The Ge amount and layer thickness in these layers are strongly dependent on the size of the oxide openings [9, 10]. HRXRD can be easily applied on the test chip with a particular oxide opening size to measure the Ge amount. Figure 5 shows $\omega/2\theta$ rocking curves from intrinsic and B-doped SiGe layers grown selectively in a chip containing 5000 oxide openings with a size of $7 \times 7\ \mu m^2$. Two more rocking curve measurements have also been performed on a $7 \times 7\ mm^2$ reference opening on the same wafers. There is a remarkable variation of the Ge amount between reference (18%) and the device openings (24%) for the intrinsic sample, which is due to the loading effect during the epitaxial process. The shift of the doped layer peaks compared to the intrinsic ones is converted to a boron concentration of 1×10^{20} and $2 \times 10^{20}\ cm^{-3}$ for reference and device opening, respectively. These measurements are fast, and they can be performed on a variety of arrays on a wafer at different process stages in the clean room. Any out-diffusion of dopants can be detected and an appropriate thermal budget of the device processing can be determined.

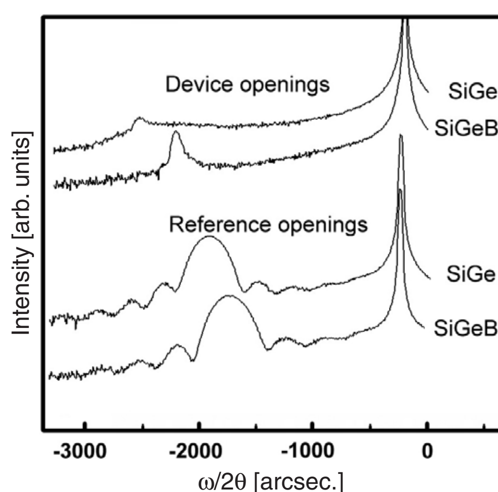

Figure 5. (004) rocking curves of intrinsic and B-doped SiGe layers grown on a patterned substrates with chips consisting of 5000 10 × 10 μm^2 oxide openings. Reference openings of 7 × 7 mm^2 were also available on each wafer.

8. Conclusions

High-resolution reciprocal lattice mapping were applied to distinguish defects such as precipitates, stacking faults and dislocations in SiGeC layers. The results showed that the precipitates caused a diffused scattering around the layer peak, whereas the extended defects created an asymmetric feature in maps. The defect density profile in SiGe/Si multilayers can be obtained by reciprocal lattice mapping around the (113), (224) and (115) reflections. Because of the low incident angle of the x-ray beam, the (113) maps demonstrated the most sensitivity to defects situated near the surface. Qualifying the defect density below the detection limit of x-ray analysis was performed by investigating the thermal stability of the SiGe layers. It has been shown that layers with higher defect density have poorer thermal stability and they can be ranked by the induced scattering around the SiGe layer peak. Substitutional carbon and boron in SiGe layers was estimated from the strain compensation amount in SiGe matrix by measuring the shift of the layer peaks in x-ray scans. X-ray measurements can be used as in-line process monitoring for layers grown in small oxide openings on patterned substrates.

References

[1] Hackbarth T, Zeuner M and König U 2002 The future of SiGe beyond HBT applications *Compound Semiconductor* **8** 45

[2] Fewster P F and Andrew N L 1993 Determining the lattice relaxation in semiconductor layer systems by x-ray diffraction *J. Appl. Phys.* **74** 3121

[3] van der Sluis P 1993 Determination of strain in epitaxial semiconductor layers by high-resolution x-ray diffraction *J. Phys. D: Appl. Phys.* **26** 188

[4] Mi J, Warren P, Gailhanou M, Ganière J-D, Dutoit M, Jouneau P-H and Houriet R 1996 Epitaxial growth of SiGeC alloy layers on (100) Si by rapid thermal chemical vapor deposition using methylsilane *J. Vac. Sci. Technol.* B **14** 1660

[5] Radamson H H, Joelsson K B, Ni W-X, Hultman L and Hansoon G V 1995 Characterization of highly boron-doped Si, Si_{1-x}/Ge_x and Ge layers by high-resolution transmission electron microscopy *J. Cryst. Growth* **157** 80

[6] Bugiel E, Ruvimov S and Osten H J 1996 TEM analysis of structure modification induced by additional carbon incorporation in silicon and SiGe layers grown with MBE *Solid State Phenom.* **47** 595

[7] Ayers J E 1994 The measurement of threading dislocation densities in semiconductor crystals by X-ray diffraction *J. Cryst. Growth* **135** 71

[8] Menon C, Radamson H H and Landgren G 2000 High quality SiGe epitaxial layer grown by RPCVD using dichlorosilane *ASDAM 2000: Conf. Proc. 3rd Int. EuroConf. on Advanced Semiconductor Devices and Microsystems* p 201

[9] Bodnar S, De Berranger E, Bouillon P, Mouis M, Skotnicki T and Regolini J L 1997 Selective Si and SiGe epitaxial heterostructures grown using an industrial low-pressure chemical vapor deposition module *J. Vac. Sci. Technol.* **15** 712

[10] Hållstedt J, Suvar E, Menon C, Hellström P-E, Östling M and Radamson H H 2004 Methods to reduce the loading effect in selective and non-selective epitaxial growth of SiGeC layers *Mater. Sci. Eng.* B **109** 122